Letters in Applied NanoBioScience
Open-Access Journal (ISSN: 2284-6808)

Article
Volume 13, Issue 4, 2024, 174
https://doi.org/10.33263/LIANBS134.174

Theoretical Studies Revealing Mitochondrial-Targeted Anticancer Activity of Oxovanadium (V) Complexes

Manos C. Vlasiou [1,*]

[1] School of Veterinary Medicine, University of Nicosia, 2414, Nicosia, Cyprus
* Correspondence: vlasiou.m@unic.ac.cy;

Scopus Author ID 56019849700
Received: 29.08.2023; Accepted: 7.07.2024; Published: 27.08.2024

Abstract: In recent years, more oxovanadium (IV/V) compounds have been tested for their cytotoxicity, with most of them having great results. Some biological evaluations of these complexes revealed several mechanisms of this activity, with most agreeing on ROS formation and mitochondria-targeted cell arrest apoptosis. Here, to evaluate the anticancer mechanism of oxovanadium (V) complexes, we used two oxovanadium (V) hydroquinone compounds with proven cytotoxicity on MDA-MB-231 breast cancer cisplatin resistance cells. This theoretical investigation showed inhibition of mitochondrial proteins and ROS generation as potential anticancer mechanisms of the oxovanadium (V) complexes.

Keywords: Oxovanadium complexes; anticancer activity; ROS generation; mitochondria.

1. Introduction

The biological role of vanadium varies in a broad spectrum of pharmacological properties in plants and animals [1]. This transition state element can be found mainly in the mammalian body in the liver, kidney, and bones [2]. As far as now, several vanadate's (V) and vanadyl (IV) derivatives presented anti-diabetic activity [3], cardioprotective activity [4], and antitumor properties in different cancer lines cells [5], even in *cisplatin* resistance breast cancer cells [6]. In addition to this, vanadium compounds are considered the next generation of metal-based antitumor agents [7].

Researchers described many mechanisms that are responsible for the inhibition of the cell cycle in cancer cells. In particular, ROS generation is the cause of a series of cellular effects triggering apoptosis, such as DNA cleavage and oxidative damage [8]. Additionally, mitochondrial localization is essential for avoiding the nuclear repair pathway and reducing the activity of the nuclear DNA targeting cytotoxic drugs [9]. Others believe any stress generated in the endoplasmic reticulum can cause cell death involving the mitochondria [10]. In other words, targeting mitochondria over the nucleus avoids mutation and damage to nuclear DNA [11].

The chelation of vanadium compounds by organic compounds is improving their pharmacological profile over simple vanadium salts [12]. The increase in vanadium lipophilicity and gastrointestinal absorption enhances this pharmacological profile [13]. Thus, the impact of vanadium-based compounds on cell cycle progression has been reported in prostate cancer cells, causing G_2/M cell cycle arrest [14]. Other studies have shown G_0/G_1 phase cell cycle arrest in human neuroblastoma cells induced by organic vanadium complexes

[15]. Moreover, cell cycle arrest in the S phase was determined in esophageal squamous carcinoma cell lines treated with sodium vanadate [16].

Molecular docking, as a computational strategy, can predict the binding site of the target protein while at the same time being able to discriminate the types of interactions between the target and the inhibitor [17]. This stationary docking, though, needs to be evaluated by *in vitro* studies, re-docking of the inhibitor to reproduce the co-crystallized binding geometry of the ligand, or by running molecular dynamics simulations [18]. Molecular dynamics (MD) is the better choice if the work is theoretical, as the particle motion is simulated according to the equations of motion. Density Functional Theory (DFT) uses the influence of an external electric field on the reactivity, predicting the reactivity and stability of the compounds [19]. So, using *in silico* methods can reveal the mechanism of the anticancer activity of metal-based compounds.

This work used various theoretical and computational approaches to understand the anticancer mechanism of two oxovanadium (V) hydroquinone complexes. In previous work from our laboratory [6], these two complexes revealed an anticancer activity on MDA-MB-231 breast cancer *cisplatin* resistance cells. Using theoretical studies, we now indicate mitochondrial targeting and ROS-mediated generation activity of these two oxovanadium (V) complexes.

2. Materials and Methods

Energy minimization is critical to determining the proper atomic arrangement in space [20]. This is because the drawn chemical structures are not energetically favorable. When the molecule is geometrically optimized, it attains the most stable conformation. Of course, the steepest descent method relies on an approximation. This technique is called ‘’Steepest Descent’’ because the direction in which the geometry is first minimized is opposite to the direction in which the gradient is most significant at the initial point [21]. At first, a minimum in the first direction is reached, and then a second minimization starts moving in the steepest remaining direction. Energy minimization was performed for the VO (V) complexes and the DNA dodecamer structure using YASARA software [22,23]. The energy minimization was done using the 500 steepest descent steps with a 0.02 Å step size and an update interval of 10.

Molecular dynamics (MD) can simulate several hundreds of atoms to systems with biological relevance, including proteins in solution with explicit solvent representations, membrane-embedded proteins, or large macromolecular complexes like ribosomes [24]. Force fields are complex equations, but they are easy to calculate. Force-field equations represent atoms as spheres and bonds as springs for bond length and angles [25]. Periodic functions for bond rotations, Lennard–Jones potentials, and Coulomb’s law for van der Waals and electrostatic interactions ensure that energy and force calculations are high-speed even for large systems [26]. Once the forces acting on individual atoms are obtained, Newton’s law of motion calculates accelerations and velocities and updates the atom positions [27]. MD simulation was performed using YASARA software to explore the interaction between the DNA (PDB: 1BNA) dodecamer structure and VO(V) complexes. During the simulation, the AMBER 96 force field was utilized. The "Berendsen thermostat" temperature coupling algorithm and the "manometer" pressure coupling algorithm were used to maintain a constant pressure (107 Pa) and temperature (25°C) during the simulation. The model and other molecules were wrapped in a periodic standard cubic box, and the complex was placed in the center of the box [28].

Molecular docking uses computation methods to predict the ligand-receptor complex structure [29]. Docking can be achieved through two interconnected steps: first, by sampling conformations of the ligand in the protein's active site and, later, by ranking these conformations via a scoring function [30]. Molecular docking studies were administered by using iGEMDOCK 2.1 software. The protein-coded crystal structures were selected from the Protein Data Bank. The novel ligands were drawn with the help of ChemDraw Ultra 12.0 and Chem3D Pro 12.0 software.

Density functional theory (DFT) is a quantum-mechanical (QM) method used in chemistry to calculate the electronic structure of atoms and molecules [31]. The real forte of DFT is a favorable price/performance ratio compared with electron-correlated wave function-based methods such as Møller–Plesset perturbation theory or coupled cluster [32]. So, larger molecular systems can be studied with sufficient accuracy, expanding in this way the predictive power inherent in electronic structure theory. Density functional theory studies were performed to obtain thermodynamic properties and to verify that each optimization achieved an energy minimum [33]. The quantum chemical descriptors extracted directly from the ORCA output file were total energy, Huckel atomic charges, electronic density, dipole moment, Mayer population analysis, the energy of the highest occupied molecular orbital (HOMO), and the energy of the lowest unoccupied molecular orbital (LUMO) [34].

3. Results and Discussion

Our first approach was to evaluate the anticancer activity of the two oxovanadium (V) hydroquinone compounds in correlation with DNA binding. We know that *cisplatin*, carboplatin, and oxaliplatin act by synthesizing DNA-platinum adducts, inducing DNA damage response [35]. Our oxovanadium (V) complexes (VOL1 and VOL2) had cytotoxic activity on MDA-MB-231 breast cancer cisplatin resistance cells. So, the first impression is that these molecules follow a different cytotoxic pathway. To prove that, we used molecular dynamics studies interacting the vanadium (V) complexes with the DNA dodecamer structure using YASARA software. The complexes cannot interact or adduct to the DNA double helix since the oxidation state (V) forms very stable complexes that cannot easily dissociate the metal ion. This fact can be witnessed in Figure 1, where complexes are not interacting with the DNA ladder in the screenshots of the simulation box.

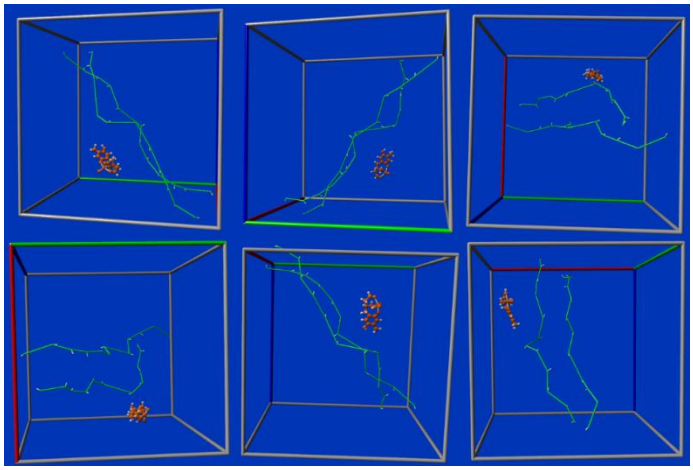

Figure 1. Screenshots of the simulation box of the molecular dynamics studies trying to interact with the DNA molecule with the cytotoxic oxovanadium complexes.

Receptor protein kinases play a crucial role in regulating cell growth and differentiation. The epidermal growth factor receptor (EGFR) also participates in cell division and differentiation among the growth factor receptor kinases [36]. This is why the research community uses kinases as primary targets to design inhibitors for anticancer therapy. In this work, following this path, we contacted molecular docking studies for eleven possible kinase targets taken from the literature (PDB: 1M17, 1S9J, 2EWA, 2HYY, 2JDR, 3D4Q, 3JVR, 3M59, 4GV1, 4JPS, 4R3P) [37]. We selected eight inhibitor candidates in clinical trials as kinase inhibitors to compare our results with our vanadium compounds from the literature (imatinib, nilotinib, dasatinib, vemurafenib, erlotinib, bosutinib, sorafenib, ibrutinib) [37]. The molecular docking studies showed that these inhibitors (in clinical trials) had better binding affinities than the vanadium complexes at all targets. This was an additional clue that the cytotoxic activity of our compounds was not because of kinase inhibition. In Table 1, we can see the binding affinities of the vanadium complexes compared with the clinical trial molecules.

Table 1. Binding affinities of the studied molecules with the target proteins (kinases).

Protein kinases targets	Inhibitor candidates	Binding affinities (KJ/mol)
1M17	VOL1	-73.98
	VOL2	-85.90
	imatinib	-100.41
	nilotinib	-104.07
	dasatinib	-97.49
	vemurafenib	-98.25
	erlotinib	-88.91
	bosutinib	-110.32
	sorafenib	-94.40
	ibrutinib	-100.34
1S9J	VOL1	-77.61
	VOL2	-79.97
	imatinib	-102.12
	nilotinib	-106.34
	dasatinib	-116.77
	vemurafenib	-115.21
	erlotinib	-95.00
	bosutinib	-124.28
	sorafenib	-111.77
	ibrutinib	-123.09
2EWA	VOL1	-77.73
	VOL2	-75.92
	imatinib	-103.41
	nilotinib	-99.83
	dasatinib	-115.30
	vemurafenib	-104.55
	erlotinib	-101.41
	bosutinib	-107.86
	sorafenib	-97.49
	ibrutinib	-111.76
2HYY	VOL1	-84.59
	VOL2	-87.24
	imatinib	-104.22
	nilotinib	-116.02
	dasatinib	-125.99
	vemurafenib	-97.13
	erlotinib	-85.05
	bosutinib	-92.40
	sorafenib	-126.93
	ibrutinib	-119.75
2JDR	VOL1	-84.28
	VOL2	-89.96
	imatinib	-79.54
	nilotinib	-83.62
	dasatinib	-78.56
	vemurafenib	-85.20
	erlotinib	-82.81

Protein kinases targets	Inhibitor candidates	Binding affinities (KJ/mol)
	bosutinib	-87.24
	sorafenib	-73.94
	ibrutinib	-88.25
3D4Q	VOL1	-81.61
	VOL2	-88.99
	imatinib	-112.63
	nilotinib	-100.03
	dasatinib	-104.81
	vemurafenib	-112.00
	erlotinib	-97.98
	bosutinib	-112.63
	sorafenib	-102.04
	ibrutinib	-117.05
3JVR	VOL1	-73.33
	VOL2	-77.83
	imatinib	-76.02
	nilotinib	-96.55
	dasatinib	-93.72
	vemurafenib	-90.53
	erlotinib	-76.59
	bosutinib	-83.32
	sorafenib	-83.02
	ibrutinib	-102.80
3M59	VOL1	-76.80
	VOL2	-77.87
	imatinib	-87.47
	nilotinib	-99.24
	dasatinib	-98.45
	vemurafenib	-101.88
	erlotinib	-82.32
	bosutinib	-94.95
	sorafenib	-91.19
	ibrutinib	-116.00
4GV1	VOL1	-78.91
	VOL2	-75.5
	imatinib	-71.85
	nilotinib	-75.82
	dasatinib	-73.16
	vemurafenib	-81.74
	erlotinib	-86.00
	bosutinib	-71.05
	sorafenib	-82.11
	ibrutinib	-79.71
4JPS	VOL1	-75.47
	VOL2	-84.85
	imatinib	-96.17
	nilotinib	-102.03
	dasatinib	-104.07
	vemurafenib	-93.00
	erlotinib	-116.27
	bosutinib	-97.97
	sorafenib	-93.72
	ibrutinib	-102.41
4R3P	VOL1	-83.55
	VOL2	-76.97
	imatinib	-102.17
	nilotinib	-107.86
	dasatinib	-91.27
	vemurafenib	-102.26
	erlotinib	-102.02
	bosutinib	-120.24
	sorafenib	-87.84
	ibrutinib	-101.74

The third approach was to evaluate the biological effect of the vanadium complexes in the mitochondrion. Extensive research on mitochondria processes in cancer indicated a crucial role in cell growth and survival [38]. So, the active redox character of our cytotoxic vanadium

compounds could target the functional mitochondria organelle. To prove that, we first needed to evaluate our complexes on several mitochondria proteins (PDB: 1H6V, 4LVT, 7EKM, 4AYX, 6O0K, 3EMN) as inhibitors using molecular docking and molecular dynamics techniques and simultaneously confirm their ROS formation activity using density functional theory studies [39 - 41].

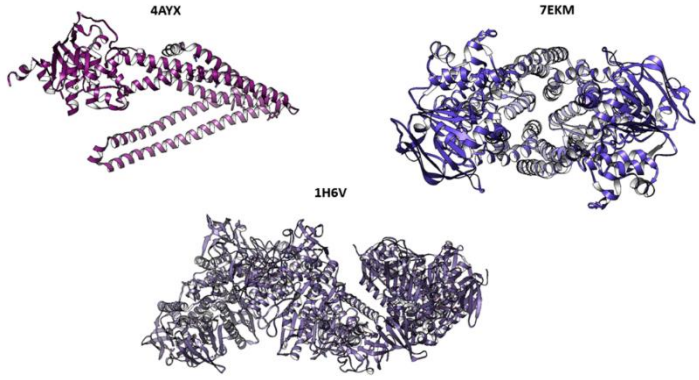

Figure 2. 3D structures of three (PDB: 4AYX, 7EKM, 1H6V) mitochondrial protein targets.

Both vanadium complexes showed high binding affinities and potent inhibition in mitochondria proteins (7EKM- Mitochondrial outer membrane protein, 1H6V- thioredoxin reductase, 4AYX- mitochondrial ABC transporter). Especially interesting is the strong binding affinity of the oxovanadium complexes on the ABC transporter since overexpression of ATP (ABC) transporters is a major contributing factor resulting in multiple drug resistance [42]. Another clue, in agreement with our previous published work, is that these complexes were cytotoxic, even in cisplatin-resistant breast cancer cells. In Figure 2, we can see the structure of 7EKM, 1H6V, and 4AYX mitochondrial proteins, and in Figure 3, we see screenshots of the molecular dynamics simulations of mitochondrial proteins with the VOL1 complex.

Table 2. Binding affinities and amino acid residues of the studied oxovanadium complexes with mitochondrial proteins.

Mitochondria target proteins	Cytotoxic metal complexes	Binding Affinities (KJ/mol)	Amino Acid Residues
1H6V	**VOL1**	**-106.61**	GLY20, SER20, ASP42, THR58, ASP334, GLY21, SER22
	VOL2	**-109.01**	GLY20, ASP42, THR58, ASP34, GLY21, SER22
4LVT	VOL1	-73.17	ASP100, ARG104, GLY142, ALA97, ASP100
	VOL2	-79.96	PHE109, LEU134, PHE101, ASP108, PHE109, MET112
7EKM	VOL1	**-94.96**	ALA627, GLY628, LYS629, SER630, ARG634
	VOL2	-67.86	ASN390, THR394, TYR550
4AYX	VOL1	**-95.99**	GLY530, SER531, GLY532, LYS533, SER534, SER529
	VOL2	-80.73	GLY530, SER531, GLY532, LYS533, SER529, GLY530, SER534
6O0K	VOL1	-79.67	TYR18, LEU95, THR96, LEU97
	VOL2	-79.21	PHE112, LEU137, PHE104
3EMN	VOL1	-64.41	ASN183, GLY192, SER193, ASN207, HIS181, GLY191
	VOL2	-65.11	HIS181, SER193, TYR195, GLN179, LEU180, ILE194

Table 3. Quantum molecular descriptors of the two oxovanadium cytotoxic complexes.

Quantum molecular descriptors	[VO(*L_1)]	[VO(*L_2)]
χ	-0.4643	-0.4371
μ	0.4643	0.4371
n	-0.4643	-0.4371
ω	-0.2322	-0.2466
E_{HOMO}	-13.1073	-12.9122
E_{LUMO}	-12.1787	-12.0380
E_{gap}	-0.9286	-0.8742

*L1: 2-((bis(2-hydroxyethyl) amino) methyl) −5-(tert-butyl) benzene-1,4-diol

**L2: 2-((bis (2-hydroxyethyl) amino) methyl) −5- methylbenzene-1,4-diol

Figure 4 depicts a screenshot of the molecular docking evaluation of the complexes with the 7EKM protein. The binding affinities of the vanadium complexes and the amino acid residues of the mitochondrial proteins can be seen in Table 2.

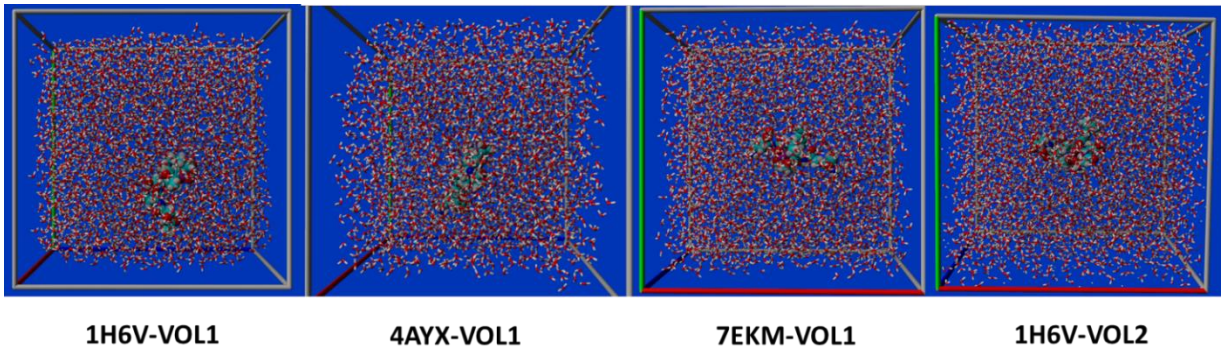

Figure 3. Simulation cells of some mitochondrial proteins interacting with VOL1 and VOL2 complex molecules.

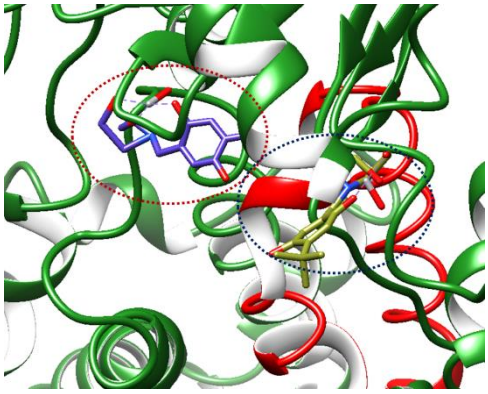

Figure 4. Screenshot of the molecular docking evaluation of the complexes with the 7EKM protein. In the red circle is the VOL1 molecule, and in the blue is the VOL2 molecule.

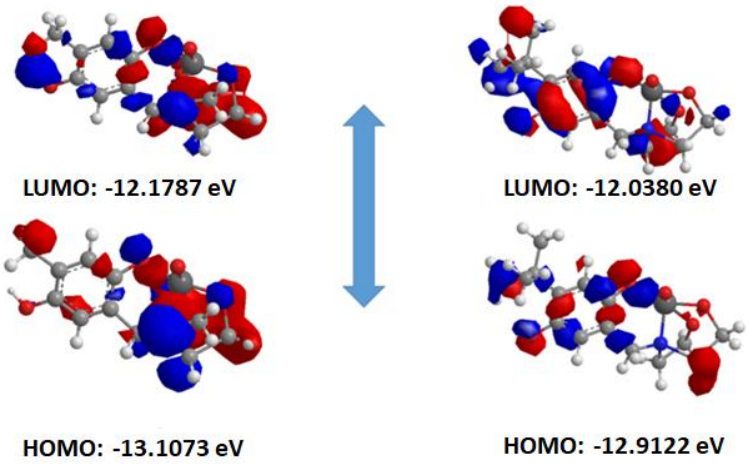

Figure 5. HOMO-LUMO orbitals of the oxovanadium cytotoxic molecules.

Their high reactivity based on the DFT studies confirms that ROS generation could promote oxidative damage to the mitochondrion. This dual action of ROS generation and mitochondria protein inhibition could be the proposed action mechanisms of the already proven cytotoxic oxovanadium (V) complexes. They are depicted in Figure 5, the HOMO-LUMO molecular orbitals of VOL1 and VOL2 vanadium complexes. Additionally, calculated quantum descriptors are in Table 3. The electrons can be transferred to molecular oxygen to $O_2^{\bullet-}$ production, and the ability of $O2^{\bullet-}$ production depends on the electron-donation capacity of the

oxovanadium complexes. The complexes drove the generation of ROS, and HOMO-LUMO gap energy (Eg = EHOMO-ELUMO) larger than the excitation energy of O_2 (approximately 0.97 eV) can be induced to $O_2^{\bullet-}$ generation [43, 44].

4. Conclusions

Herein, we have utilized *in silico* evaluation methods to look inside the cytotoxic mechanism of two oxovanadium (V) hydroquinone complexes. In particular, we used molecular dynamics, molecular docking, and density functional theory studies. The theoretical studies reveal that oxovanadium compounds can inhibit the action of mitochondrial proteins since they have strong binding affinities on them. Moreover, based on their reactivity and 'non-innocent' character, these complexes can produce ROS, another important aspect of the cytotoxic mechanism in the cancer cell's mitochondrion. Thus, this theoretical evaluation proposes a mitochondrial-targeted anticancer mechanism of oxovanadium (V) complexes.

Funding

None.

Acknowledgments

None.

Conflicts of Interest

"The authors declare no conflict of interest

References

1. Tripathi, D.; Mani, V.; Pal, R.P. Vanadium in Biosphere and Its Role in Biological Processes. *Biol. Trace Elem. Res.* **2018**, *186*, 52-67, https://doi.org/10.1007/s12011-018-1289-y.
2. Vuoti, E.; Palosaari, S.; Peräniemi, S.; Tervahauta, A.; Kokki, H.; Kokki, M.; Tuukkanen, J.; Lehenkari, P. In utero deposition of trace elements and metals in tissues. *J. Trace Elem. Med. Biol.* **2022**, *73*, 127042, https://doi.org/10.1016/j.jtemb.2022.127042.
3. Srivastava, A.K.; Mehdi, M.Z. Insulino-mimetic and anti-diabetic effects of vanadium compounds. *Diabetic Med.* **2005**, *22*, 2-13, https://doi.org/10.1111/j.1464-5491.2004.01381.x.
4. Barrio, D.A.; Etcheverry, S.B. Potential Use of Vanadium Compounds in Therapeutics. *Curr. Med. Chem.* **2010**, *17*, 3632-3642, https://doi.org/10.2174/092986710793213805.
5. Sahu, G.; Banerjee, A.; Samanta, R.; Mohanty, M.; Lima, S.; Edward, R.T.; Dinda, R. Water-soluble Dioxidovanadium (V) Complexes of Arolhydrazones: DNA/BSA Interactions, Hydrophobicity, and Cell-Selective Anticancer Potential. *Inorganic Chemistry* **2021**, *60*, 15291-15309, https://doi.org/10.1021/acs.inorgchem.1c01899.
6. Ioannou, K.; Eleftheriou, C.; Drouza, C.; Pafiti, K.S.; Panayi, T.; Keramidas, A.D.; Zacharia, L.C.; Vlasiou, M.C. Novel Zinc and Vanadium (V) Hydroquinonate Complexes: Synthesis and Biological Solution Evaluation. *J. Mol. Struct.* **2022**, *1257*, 132582, https://doi.org/10.1016/j.molstruc.2022.132582.
7. Vlasiou, M.C.; Pafiti, K.S. Cell Arrest and Apoptosis Induced by the Next Generation of Vanadium Based Drugs: Action to Mechanism Relation and Future Perspectives. *Anti-Cancer Agents Med. Chem.* **2020**, *21*, 2111-2116, https://doi.org/10.2174/1871520621666201222143839.
8. Leon, I.E.; Di Virgilio, A.L.; Porro, V.; Muglia, C.I.; Naso, L.G.; Williams, P.A.M.; Bollati-Fogolin, M.; Etcheverry, S.B. Antitumor properties of a vanadyl(iv) complex with the flavonoid chrysin $[VO(chrysin)_2EtOH]_2$ in a human osteosarcoma model: the role of oxidative stress and apoptosis. *Dalton Trans.* **2013**, *42*, 11868-11880, https://doi.org/10.1039/C3DT50524C.

9. Bhattacharyya, U.; Kumar, B.; Garai, A.; Bhattacharyya, A.; Kumar, A.; Banerjee, S.; Kondaiah, P.; Chakravarty, A.R. Curcumin "Drug" Stabilized in Oxidovanadium(IV)-BODIPY Conjugates for Mitochondria-Targeted Photocytotoxicity. *Inorg. Chem.* **2017**, *56*, 12457-12468, https://doi.org/10.1021/acs.inorgchem.7b01924.
10. Banerjee, S.; Dixit, A.; Shridharan, R.N.; Karande, A.A.; Chakravarty, A.R. Endoplasmic reticulum targeted chemotherapeutics: the remarkable photo-cytotoxicity of an oxovanadium(iv) vitamin-B6 complex in visible light. *Chem. Commun.* **2014**, *50*, 5590-5592, https://doi.org/10.1039/C4CC02093F.
11. Banik, B.; Somyajit, K.; Nagaraju, G.; Chakravarty, A.R. Oxovanadium(iv) complexes of curcumin for cellular imaging and mitochondria targeted photocytotoxicity. *Dalton Trans.* **2014**, *43*, 13358-13369, https://doi.org/10.1039/C4DT01487A.
12. León, I.E.; Butenko, N.; Di Virgilio, A.L.; Muglia, C.I.; Baran, E.J.; Cavaco, I.; Etcheverry, S.B. Vanadium and cancer treatment: Antitumoral mechanisms of three oxidovanadium(IV) complexes on a human osteosarcoma cell line. *J. Inorg. Biochem.* **2014**, *134*, 106-117, https://doi.org/10.1016/j.jinorgbio.2013.10.009.
13. McNeill, J.H.; Yuen, V.G.; Hoveyda, H.R.; Orvig, C. Bis(maltolato)oxovanadium(IV) is a potent insulin mimic. *J. Med. Chem.* **1992**, *35*, 1489-1491, https://doi.org/10.1021/jm00086a020.
14. Desoize, B. Metals and metal compounds in cancer treatment. *Anticancer Res.* **2004**, *24*, 1529-1544.
15. Yu, Q.; Jiang, W.; Li, D.; Gu, M.; Liu, K.; Dong, L.; Wang, C.; Jiang, H.; Dai, W. Sodium orthovanadate inhibits growth and triggers apoptosis of human anaplastic thyroid carcinoma cells in vitro and in vivo. *Oncol. Lett.* **2019**, *17*, 4255-4262, https://doi.org/10.3892/ol.2019.10090.
16. Kowalski, S.; Wyrzykowski, D.; Hac, S.; Rychlowski, M.; Radomski, M.W.; Inkielewicz-Stepniak, I. New Oxidovanadium(IV) Coordination Complex Containing 2-Methylnitrilotriacetate Ligands Induces Cell Cycle Arrest and Autophagy in Human Pancreatic Ductal Adenocarcinoma Cell Lines. *Int. J. Mol. Sci.* **2019**, *20*, 261, https://doi.org/10.3390/ijms20020261.
17. Vlasiou, M.C.; Ioannou, K.I.; Pafiti, K.S. Molecular Docking, DFT Studies and ADMET Simulations for Evaluating Already Approved FDA Drugs as Inhibitors for SARS-Cov-2 RNADependent Polymerase. *Lett. Drug Des. Discov.* **2021** *18*, 674–685, https://doi.org/10.2174/1570180817999201211192513.
18. Vlasiou, M.C.; Petrou, C.C.; Sarigiannis, Y.; Pafiti, K.S. Density Functional Theory Studies and Molecular Docking on Xanthohumol, 8-Prenylnaringenin and Their Symmetric Substitute Diethanolamine Derivatives as Inhibitors for Colon Cancer-Related Proteins. *Symmetry* **2021**, *13*, 948, https://doi.org/10.3390/sym13060948.
19. Mavra, A.; Petrou, C.C.; Vlasiou, M.C. Ligand and Structure-Based Virtual Screening in Combination, to Evaluate Small Organic Molecules as Inhibitors for the XIAP Anti-Apoptotic Protein: The Xanthohumol Hypothesis. *Molecules* **2022**, *27*, 4825, https://doi.org/10.3390/molecules27154825.
20. Nimmegeers, P.; Telen, D.; Logist, F.; Impe, J.V. Dynamic optimization of biological networks under parametric uncertainty. *BMC Syst. Biol.* **2016**, *10*, 86, https://doi.org/10.1186/s12918-016-0328-6.
21. Balali-Mood, K.; Harroun, T.A.; Bradshaw, J.P. Molecular dynamics simulations of a mixed DOPC/DOPG bilayer. *Eur. Phys. J.E.* **2003**, *12*, 135–140, https://doi.org/10.1140/epjed/e2003-01-031-3.
22. Hossen, M.R.; Biswas, S.; Ali, M.A.; Halim, M.A.; Ullah, M.O. In silico peptide-based therapeutics against human colorectal cancer by the activation of TLR5 signaling pathways. *J. Mol. Model.* **2023**, *29*, 35, https://doi.org/10.1007/s00894-022-05422-2.
23. Evadgian, A.; Bharatha, A.; Cohall, D. Use of Cheminformatics to Determine Potential Drug Interactions between Popular Barbadian Botanical Medicines and Antihypertensive Drugs. *ACS Omega* **2022**, *7*, 44603–44619, https://doi.org/10.1021/acsomega.2c02446.
24. Greene, D.A.; Qi, R.; Nguyen, R.; Qiu, T.; Luo, R. Heterogeneous Dielectric Implicit Membrane Model for the Calculation of MMPBSA Binding Free Energies. *J. Chem. Inf. Model.* **2019**, *59*, 3041–3056, https://doi.org/10.1021/acs.jcim.9b00363.
25. Bardena, D.R.; Vashisth, H. Parameterization and atomistic simulations of biomimetic membranes. *Faraday Discuss.* **2018**, *209*, 161-178, https://doi.org/10.1039/C8FD00047F.
26. Elking, D.M.; Perera, L.; Duke, R.; Darden, T.; Pedersen, L.G. Atomic forces for geometry-dependent point multipole and Gaussian multipole models. *J. Comput. Chem.* **2010**, *31*, 2702-2713, https://doi.org/10.1002/jcc.21563.
27. Wang, L.; Lee, J.D. Temperature and entropy in molecular system. *J. Micromech. Mol. Phys.* **2022**, *7*, 17-27, https://doi.org/10.1142/S2424913021420054.

28. Krieger, E.; Vriend, G.; New ways to boost molecular dynamics simulations. *J. Comput. Chem.* **2015**, *36*, 996-1007, https://doi.org/10.1002/jcc.23899.
29. Hariono, M.; Wijaya, D.B.E.; Chandra, T.; Frederick, N.; Putri, A.B.; Herawati, E.; Warastika, L.A.; Permatasari, M.; Putri, A.D.A.; Ardyantoro, S. A Decade of Indonesian Atmosphere in Computer-Aided Drug Design. *J. Chem. Inf. Model.* **2022**, *62*, 5276–5288, https://doi.org/10.1021/acs.jcim.1c00607.
30. Ito, S.; Yagi, K.; Sugita, Y. Computational Analysis on the Allostery of Tryptophan Synthase: Relationship between α/β-Ligand Binding and Distal Domain Closure. *J. Phys. Chem. B.* **2022**, *126*, 3300–3308, https://doi.org/10.1021/acs.jpcb.2c01556.
31. Rodrigues, J.L.; Ligorio, R.F.; Krawczuk, A.; Diniz, R.; Dos Santos, L.H.R. Distributed functional-group polarizabilities in polypeptides and peptide clusters toward accurate prediction of electro-optical properties of biomacromolecules. *J. Mol. Model.* **2023**, *29*, 49, https://doi.org/10.1007/s00894-023-05451-5.
32. Sharma, M.; Sierka, M. Efficient Implementation of Density Functional Theory Based Embedding for Molecular and Periodic Systems Using Gaussian Basis Functions. *J. Chem. Theory Comput.* **2022**, *18*, 6892–6904, https://doi.org/10.1021/acs.jctc.2c00380.
33. Gibney, D.; Boyn, J.-N.; Mazziotti, D.A. Density Functional Theory Transformed into a One-Electron Reduced-Density-Matrix Functional Theory for the Capture of Static Correlation. *J. Phys. Chem. Lett.* **2022**, *13*, 1382–1388, https://doi.org/10.1021/acs.jpclett.2c00083.
34. Choudhary, V.K.; Mandhan, K.; Dash, D.; Bhardwaj, S.; Kumari, M.; Sharma, N. Density functional theory studies on molecular geometry, spectroscopy, HOMO–LUMO and reactivity descriptors of titanium(IV) and oxidozirconium(IV) complexes of phenylacetohydroxamic acid. *J. Comput. Chem.* **2022**, *43*, 2060-2071, https://doi.org/10.1002/jcc.27004.
35. Li, R.; Zhao, W.; Jin, C.; Xiong, H. Dual–target platinum(IV) complexes reverse cisplatin resistance in triple negative breast via inhibiting poly(ADP–ribose) polymerase (PARP–1) and enhancing DNA damage. *Bioinorg. Chem.* **2023**, *133*, 106354, https://doi.org/10.1016/j.bioorg.2023.106354.
36. Kumar, C.B.P.; Raghu, M.S.; Prathibha, B.S.; Prashanth, M.K.; Kanthimathi, G.; Kumar, K.Y.; Parashuram, L.; Alharthi, F.A. Discovery of a novel series of substituted quinolines acting as anticancer agents and selective EGFR blocker: Molecular docking study. *Bioorg. Med. Chem. Lett.* **2021**, *44*, 128118, https://doi.org/10.1016/j.bmcl.2021.128118.
37. Gagic, Z.; Ruzic, D.; Djokovic, N.; Djikic, T.; Nikolic, K. *In silico* Methods for Design of Kinase Inhibitors as Anticancer Drugs. *Front. Chem.* **2020**, *7*, 873, https://doi.org/10.3389/fchem.2019.00873.
38. Olelewe, C.; Awuah, S.G. Mitochondria as a target of third-row transition metal-based anticancer complexes. *Curr. Opin. Chem. Biol.* **2023**, *72*, 102235, https://doi.org/10.1016/j.cbpa.2022.102235.
39. Anantram, A.; Kundaikar, H.; Degani, M.; Prabhu, A. Molecular dynamic simulations on an inhibitor of anti-apoptotic Bcl-2 proteins for insights into its interaction mechanism for anti-cancer activity. *J. Biomol. Struct. Dyn.* **2019**, *37*, 3109-3121, https://doi.org/10.1080/07391102.2018.1508371.
40. Elkholi, R.; Renault, T.T.; Serasinghe, M.N.; Chipuk, J.E. Putting the pieces together: How is the mitochondrial pathway of apoptosis regulated in cancer and chemotherapy?. *Cancer Metab.* **2014**, *2*, 16, https://doi.org/10.1186/2049-3002-2-16.
41. Wang, C.; Youle, R.J. The Role of Mitochondria in Apoptosis. *Annu. Rev. Genet.* **2009**, *43*, 95–118, https://doi.org/10.1146/annurev-genet-102108-134850.
42. Zheng, Y.; Ma, L.; Sun, Q. Clinically-Relevant ABC Transporter for Anti-Cancer Drug Resistance. *Front. Pharmacol.* **2021**, *12*, 648407, https://doi.org/10.3389/fphar.2021.648407.
43. Yao, H.; Huang, Y.; Li, X.; Li, X.; Xie, H.; Luo, T.; Chen, J.; Chen, Z. Underlying mechanisms of reactive oxygen species and oxidative stress photoinduced by graphene and its surface-functionalized derivatives. *Environ. Sci.: Nano* **2020**, *7*, 782-792, https://doi.org/10.1039/C9EN01295H.
44. Schweitzer, C.; Schmidt, R. Physical Mechanisms of Generation and Deactivation of Singlet Oxygen. *Chem. Rev.* **2003**, *103*, 1685-1757, https://doi.org/10.1021/cr010371d.